DALTON
FULL PAPER

Niobium–η-cyclopentadienyl compounds with imido and amido ligands derived from 2,6-dimethylaniline

Martin J. Humphries, Malcolm L. H. Green,* Richard E. Douthwaite and Leigh H. Rees

Inorganic Chemistry Laboratory, South Parks Road, Oxford, UK OX1 3QR

Received 5th September 2000, Accepted 19th October 2000
First published as an Advance Article on the web 28th November 2000

The new niobium imido complex [Nb(η-C_5H_5){N($C_6H_3Me_2$-2,6)}Cl_2] **1*** has been prepared. Its reactions with anionic reagents lead to a series of alkyl and amido derivatives [Nb(η-C_5H_5){N($C_6H_3Me_2$-2,6)}MeCl] **2**, [Nb(η-C_5H_5){N($C_6H_3Me_2$-2,6)}{NH($C_6H_3Me_2$-2,6)}Cl] **3**, [Nb(η-C_5H_5){N($C_6H_3Me_2$-2,6)}{NH($C_6H_3Me_2$-2,6)}$_2$] **4***, [Nb(η-C_5H_5)$_2${N($C_6H_3Me_2$-2,6)}Cl] **5**, [Nb(η-C_5H_5)$_2${N($C_6H_3Me_2$-2,6)}Me] **6** and [Nb(η-C_5H_5){N($C_6H_3Me_2$-2,6)}{NH($C_6H_3Me_2$-2,6)}Me] **7***. Variable temperature NMR studies on the amido complexes **3**, **4** and **7** are reported (* indicates the crystal structure has been determined).

Introduction

Metal imido complexes are ubiquitous within the chemistry of the early transition metals. This widespread use of the imido ligand has arisen both due to its isoelectronic relationship with the cyclopentadiene ligand and the ease with which derivatives of differing bulk and electronic properties can be synthesized by variation of the group attached to the nitrogen atom.[1] High reactivity of these complexes can be achieved by synthesizing co-ordinatively unsaturated complexes containing multiple π-bonded ligands. Such "π loading" destabilises the strong metal–nitrogen π interactions and can lead to reactive imido moieties.[2]

Our recent work has centred upon the synthesis of π-loaded complexes of niobium. In the course of this work we have recently reported the synthesis of a series of niobium imido amido complexes with ligands derived from *tert*-butylamine; these proved to be of low crystallinity, similar complexes were also reported by Royo and co-workers.[3] In order further to study the structure and bonding of this type of compound we have synthesized analogous species derived from the new niobium imido compound [Nb(η-C_5H_5){N($C_6H_3Me_2$-2,6)}Cl_2].

During the course of this work related niobium species derived from [Nb{η-C_5H_4($SiMe_3$)}{N($C_6H_3Me_2$-2,6)}Cl_2] were reported,[4] as were a number of other cyclopentadienyl imido complexes.[5]

Results and discussion

The reaction between [Nb(η-C_5H_5)Cl_4][6] and [NH($SiMe_3$)($C_6H_3Me_2$-2,6)] in the presence of $NC_5H_3Me_2$-2,6, in dichloromethane afforded [Nb(η-C_5H_5){N($C_6H_3Me_2$-2,6)}Cl_2] **1** (Scheme 1) as mildly air- and moisture-sensitive red crystals that were only slightly soluble in pentane, but soluble in all other non-protic organic solvents. The data characterising **1**, and all the other new compounds **2**–**7** described in this paper, are given in Table 1.

The crystal structure of compound **1** has been determined and the molecular structure is given in Fig. 1 and selected interatomic distances and angles are listed in Table 2. The Nb(1)–N(2) distance lies in the range where the nitrogen is considered to be acting as a four electron donor, and the imido ligand is approximately linear, with the Nb(1)–N(2)–C(3) angle being 166.6(2)°. The Nb–Cl distances (2.3319(8) and 2.3433(9) Å) are comparable to those observed in other structurally characterised sixteen electron compounds of general formula [Nb(η-C_5H_5)(NR)Cl_2], in which the bonds are in the range 2.338–2.358 Å.[7,8]

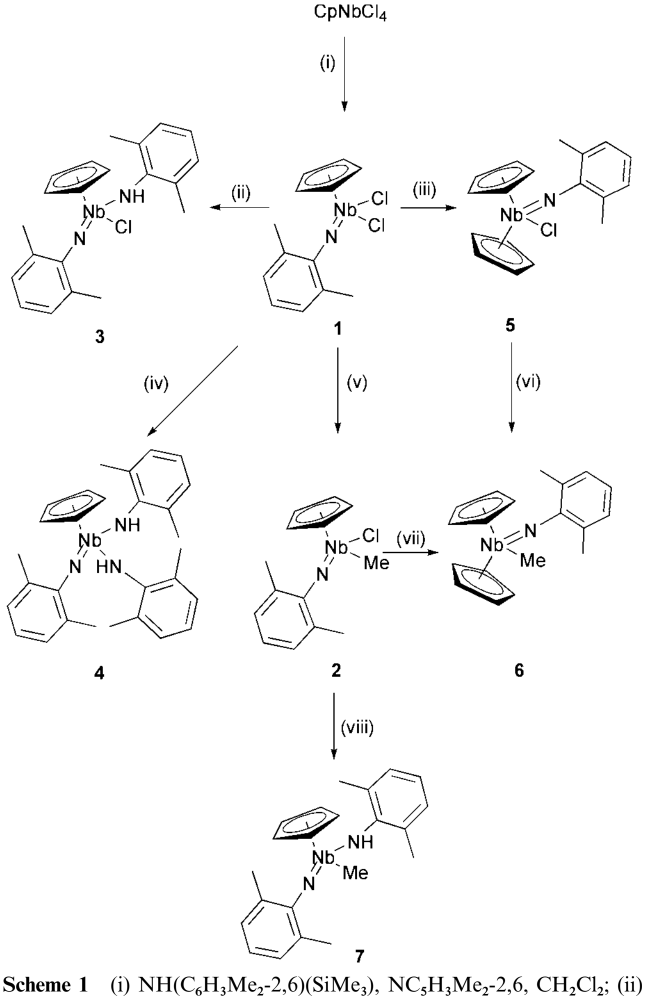

Scheme 1 (i) NH($C_6H_3Me_2$-2,6)($SiMe_3$), $NC_5H_3Me_2$-2,6, CH_2Cl_2; (ii) Li[NH($C_6H_3Me_2$-2,6)], toluene, −78 °C; (iii) Mg(C_5H_5)$_2$, THF; (iv) 2 Li[NH($C_6H_3Me_2$-2,6)], toluene, −78 °C; (v) MgMeCl, Et_2O, −78 °C; (vi) LiMe, Et_2O, −78 °C; (vii) Li(C_5H_5), THF; (viii) LiNH($C_6H_3Me_2$-2,6), toluene, −78 °C.

The cyclopentadienyl ligand is oriented such that one of its apices, C(15), nearly eclipses the Nb(1)–N(2) bond, with this Nb–C distance being the shortest. The two carbon atoms *trans* to C(15) display the longest metal–carbon distances. In

DOI: 10.1039/b007178l

Table 1 Analytical and spectroscopic data

Compound and analytical data[a]	NMR data[b]
1 $[Nb(\eta\text{-}C_5H_5)\{N(C_6H_3Me_2\text{-}2,6)\}Cl_2]$ Red crystals C 44.9 (44.9), H 4.1 (4.1), N 4.0 (4.0) MS, EI: $m/z = 347$, $(M)^+$, 100; 228 $(M - NC_6H_3Me_2)^+$, 82%	^1H: 6.78 (d, 2H, $^3J_{HH} = 7.5$, *m*-H of $C_6H_3(CH_3)_2$), 6.67 (t, 1H, $^3J_{HH} = 7.5$, *p*-H of $C_6H_3(CH_3)_2$), 5.74 (s, 5H, C_5H_5), 2.32 (s, 6H, $C_6H_3(CH_3)_2$) ^{13}C: 155.34 ($C_6H_3(CH_3)_2$), 134.98 ($C_6H_3(CH_3)_2$), 127.75 ($C_6H_3(CH_3)_2$), 125.85 ($C_6H_3(CH_3)_2$), 113.57 (C_5H_5), 19.20 ($C_6H_3(CH_3)_2$)
2 $[Nb(\eta\text{-}C_5H_5)\{N(C_6H_3Me_2\text{-}2,6)\}MeCl]$ Red crystals C 51.1 (51.3), H 5.2 (5.2), N 4.2 (4.3) MS, EI: $m/z = 327$, $(M)^+$, 42; 312 $(M - Me)^+$, 65; 193 $(M - Me - NC_6H_3Me_2)^+$, 100%	^1H: 7.01 (d, 2H, $^3J_{HH} = 7.5$, *m*-H of $C_6H_3(CH_3)_2$), 6.69 (t, 1H, $^3J_{HH} = 7.5$, *p*-H of $C_6H_3(CH_3)_2$), 5.36 (s, 5H, C_5H_5), 2.21 (s, 6H, $(CH_3)_2C_6H_3$), 0.94 (s, 3H, $NbCH_3$) $^{13}C\text{-}\{^1H\}$: 154.74 ($C_6H_3(CH_3)_2$), 134.16 ($C_6H_3(CH_3)_2$), 127.72 ($C_6H_3(CH_3)_2$), 124.37 ($C_6H_3(CH_3)_2$), 110.02 (C_5H_5), 40.16 ($NbCH_3$), 19.51 ($C_6H_3(CH_3)_2$)
3 $[Nb(\eta\text{-}C_5H_5)\{N(C_6H_3Me_2\text{-}2,6)\}\{NH(C_6H_3Me_2\text{-}2,6)\}Cl]$ Yellow solid C 58.3 (57.3), H 5.6 (5.5), N 6.5 (6.3) MS, EI: $m/z = 432$, $(M)^+$, 59; 347 $(M - C_5H_5)^+$, 19; 312 $(M - NHC_6H_3Me_2)^+$, 100%	^1H:[c] 8.97 (br s, 1H, NH), 6.98 (d, 2H, $^3J_{HH} = 7.5$, *m*-H of $NHC_6H_3(CH_3)_2$), 6.81 (d, 2H, $^3J_{HH} = 7.5$, *m*-H of $NC_6H_3(CH_3)_2$), 6.76 (t, 1H, $^3J_{HH} = 7.5$, *p*-H of $NHC_6H_3(CH_3)_2$), 6.66 (t, 1H, $^3J_{HH} = 7.5$, *p*-H of $NC_6H_3(CH_3)_2$), 5.75 (s, 5H, C_5H_5), 2.34 (br s, 6H, $NHC_6H_3(CH_3)_2$), 2.22 (br s, 6H, $NC_6H_3(CH_3)_2$) $^{13}C\text{-}\{^1H\}$:[d] 155.03 ($C_6H_3(CH_3)_2$), 152.88 ($C_6H_3(CH_3)_2$), 137.45 ($C_6H_3(CH_3)_2$), 134.24 ($C_6H_3(CH_3)_2$), 129.87 ($C_6H_3(CH_3)_2$), 128.68 ($C_6H_3(CH_3)_2$), 124.41 ($C_6H_3(CH_3)_2$), 124.37 ($C_6H_3(CH_3)_2$), 110.70 (C_5H_5), 20.15 ($C_6H_3(CH_3)_2$), 19.51 ($C_6H_3(CH_3)_2$)
4 $[Nb(\eta\text{-}C_5H_5)\{N(C_6H_3Me_2\text{-}2,6)\}\{NH(C_6H_3Me_2\text{-}2,6)\}_2]$ Yellow crystals C 66.9 (67.3), H 6.6 (6.6), N 8.0 (8.1) MS, EI: $m/z = 517$, $(M)^+$, 100; 397 $(M - NH(C_6H_3Me_2\text{-}2,6))^+$, 92%	^1H: 7.04 (d, 4H, $^3J_{HH} = 7.5$, *m*-H of $NHC_6H_3(CH_3)_2$), 7.03 (br s, 2H, NH), 6.88 (t, 2H, $^3J_{HH} = 7.5$, *m*-H of $NC_6H_3(CH_3)_2$), 6.80 (d, 2H, $^3J_{HH} = 7.5$, *p*-H of $NHC_6H_3(CH_3)_2$), 6.65 (t, 1H, $^3J_{HH} = 7.5$, *p*-H of $NC_6H_3(CH_3)_2$), 5.61 (s, 5H, C_5H_5), 2.36 (s, 12H, $NHC_6H_3(CH_3)_2$), 2.04 (s, 6H, $NC_6H_3(CH_3)_2$) ^{13}C: 155.12 ($C_6H_3(CH_3)_2$), 154.52 ($C_6H_3(CH_3)_2$), 133.76 ($C_6H_3(CH_3)_2$), 128.80 ($C_6H_3(CH_3)_2$), 127.66 ($C_6H_3(CH_3)_2$), 127.50 ($C_6H_3(CH_3)_2$), 123.69 ($C_6H_3(CH_3)_2$), 121.84 ($C_6H_3(CH_3)_2$), 109.33 (C_5H_5), 20.56 ($C_6H_3(CH_3)_2$), 18.98 ($C_6H_3(CH_3)_2$)
5 $[Nb(\eta\text{-}C_5H_5)_2\{N(C_6H_3Me_2\text{-}2,6)\}Cl]$ Red crystals C 56.9 (57.2), H 5.3 (5.1), N 3.6 (3.7) MS, EI: $m/z = 377$, $(M)^+$, 52; 321, $(M - Cp)^+$, 29; 265 $(M - NC_6H_3Me_2)^+$, 33%	^1H: 6.94 (d, 2H, $^3J_{HH} = 7.5$, *m*-H of $C_6H_3(CH_3)_2$), 6.67 (t, 1H, $^3J_{HH} = 7.5$, *p*-H of $C_6H_3(CH_3)_2$), 5.68 (s, 10H, C_5H_5), 2.25 (s, 6H, $C_6H_3(CH_3)_2$) ^{13}C: 157.84 ($C_6H_3(CH_3)_2$), 128.12 ($C_6H_3(CH_3)_2$), 127.87 ($C_6H_3(CH_3)_2$), 121.74 ($C_6H_3(CH_3)_2$), 112.99 (C_5H_5), 19.76 ($C_6H_3(CH_3)_2$)
6 $[Nb(\eta\text{-}C_5H_5)_2\{N(C_6H_3Me_2\text{-}2,6)\}Me]$ Orange crystals C 63.4 (63.9), H 6.4 (6.2), N 3.7 (3.9) MS, EI: $m/z = 357$, $(M)^+$, 79; 321, $(M - Me)^+$ 100; 223, $(M - Me - NC_6H_3Me_2)^+$, 33%	^1H: 7.01 (d, 2H, $^3J_{HH} = 7.5$, *m*-H of $C_6H_3(CH_3)_2$), 6.93 (t, 1H, $^3J_{HH} = 7.5$, *p*-H of $C_6H_3(CH_3)_2$), 5.37 (s, 10H, C_5H_5), 2.40 (s, 6H, $C_6H_3(CH_3)_2$), 0.98 (s, 3H, $NbCH_3$) ^{13}C: 157.74 ($C_6H_3(CH_3)_2$), 127.78 ($C_6H_3(CH_3)_2$), 127.02 ($C_6H_3(CH_3)_2$), 108.83 (C_5H_5), 19.90 ($C_6H_3(CH_3)_2$), 10.10 (br, CH_3)
7 $[Nb(\eta\text{-}C_5H_5)\{N(C_6H_3Me_2\text{-}2,6)\}\{NH(C_6H_3Me_2\text{-}2,6)\}Me]$ Yellow crystals C 63.9 (64.1), H 6.1 (6.1), N 6.7 (6.8) MS, EI: $m/z = 412$, $(M)^+$, 46; 397 $(M - Me)^+$, 100%	^1H: 8.18 (br s, 1H, NH), 6.97 (d, 2H, $^3J_{HH} = 7.5$, *m*-H of $C_6H_3(CH_3)_2$), 6.96 (d, 2H, $^3J_{HH} = 7.5$, *m*-H of $C_6H_3(CH_3)_2$), 6.85 (t, 1H, $^3J_{HH} = 7.5$, *p*-H of $C_6H_3(CH_3)_2$), 6.78 (t, 1H, $^3J_{HH} = 7.5$, *p*-H of $C_6H_3(CH_3)_2$), 5.74 (s, 5H, C_5H_5), 2.35 (s, 6H, $NC_6H_3(CH_3)_2$), 2.15 (s, 6H, $NHC_6H_3(CH_3)_2$), 1.01 (s, 3H, $NbCH_3$) ^{13}C: 155.10 ($C_6H_3(CH_3)_2$), 152.51 ($C_6H_3(CH_3)_2$), 133.77 ($C_6H_3(CH_3)_2$), 129.52 ($C_6H_3(CH_3)_2$), 128.51 ($C_6H_3(CH_3)_2$), 127.69 ($C_6H_3(CH_3)_2$), 123.30 ($C_6H_3(CH_3)_2$, 122.97 ($C_6H_3(CH_3)_2$), 108.36 (C_5H_5), 21.40 (br., CH_3), 19.99 ($C_6H_3(CH_3)_2$), 19.70 ($C_6H_3(CH_3)_2$)

[a] Calculated values given in parentheses. [b] NMR data are given as chemical shift (δ) (multiplicity, relative intensity, J/Hz, assignment). [c] In $C_6D_5CD_3$ at 80 °C. [d] In $C_6D_5CD_3$.

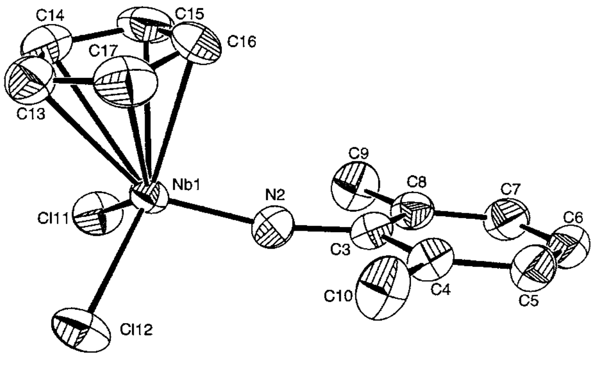

Fig. 1 The molecular structure of $[Nb(\eta\text{-}C_5H_5)\{N(C_6H_3Me_2\text{-}2,6)\}Cl_2]$ **1**. Hydrogen atoms have been omitted for clarity.

Table 2 Selected interatomic distances (Å) and angles (°) for $[Nb(\eta\text{-}C_5H_5)\{N(C_6H_3Me_2\text{-}2,6)\}Cl_2]$ **1**

Nb(1)–N(2)	1.763(2)	Nb(1)–C(14)	2.487(3)
N(2)–C(3)	1.375(4)	Nb(1)–C(15)	2.378(3)
Nb(1)–Cl(11)	2.3319(8)	Nb(1)–C(16)	2.347(3)
Nb(1)–Cl(12)	2.3433(9)	Nb(1)–C(17)	2.384(3)
Nb(1)–C(13)	2.486(3)	C(13)–C(14)	1.373(5)
C(14)–C(15)	1.408(5)	C(15)–C(16)	1.391(5)
C(16)–C(17)	1.389(5)	C(13)–C(17)	1.389(5)
Nb(1)–N(2)–C(3)	166.6(2)	Cl(11)–Nb(1)–Cl(12)	107.57(4)
N(2)–Nb(1)–Cl(11)	103.85(8)	N(2)–Nb(1)–Cl(12)	107.57(4)

addition the bond between the two *trans* carbons is the shortest in the cyclopentadienyl ring. These features of cyclopentadienyl ring bonding are also observed in the compounds $[Re(\eta\text{-}C_5H_5)(N^tBu)Cl_2]$[9] and $[Nb(\eta\text{-}C_5H_5)(NMe)Cl_2]$.[10] The compound $[Nb(\eta\text{-}C_5H_5)\{N(C_6H_3{}^iPr_2\text{-}2,6)\}Cl_2]$ has a similar arrangement of the niobium–carbon bonds, but the C–C bond *trans* to the niobium–imido bond is the longest in this instance.[7]

The reaction between $[Nb(\eta\text{-}C_5H_5)\{N(C_6H_3Me_2\text{-}2,6)\}Cl_2]$ **1** and MeMgCl at −78 °C, in diethyl ether afforded air- and moisture-sensitive red crystals of $[Nb(\eta\text{-}C_5H_5)\{N(C_6H_3Me_2\text{-}2,6)\}MeCl]$ **2**.

The reaction between complex **1** and a slurry of one equivalent of $LiNH(C_6H_3Me_2\text{-}2,6)$ in toluene at −78 °C, followed by slow warming to room temperature, afforded $[Nb(\eta\text{-}C_5H_5)\{N(C_6H_3Me_2\text{-}2,6)\}\{NH(C_6H_3Me_2\text{-}2,6)\}Cl]$ **3** as a highly air- and moisture-sensitive yellow powder. Despite repeated attempts to re-crystallise **3**, it was not possible to isolate the

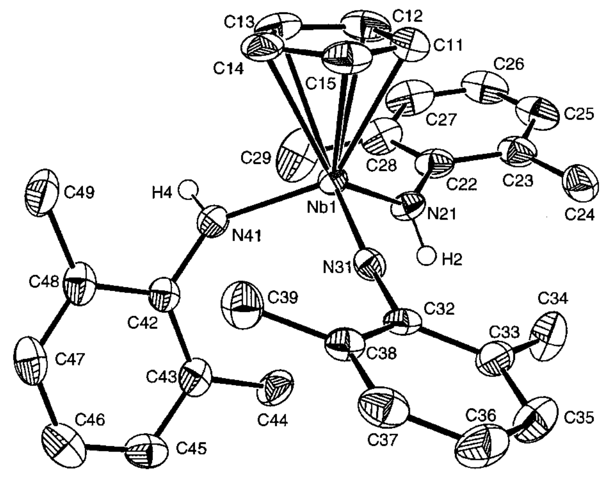

Fig. 2 The molecular structure of $[Nb(\eta\text{-}C_5H_5)\{N(C_6H_3Me_2\text{-}2,6)\}\{NH(C_6H_3Me_2\text{-}2,6)\}_2]$ **4**. The non-disordered molecule is shown. Hydrogen atoms attached to carbon have been omitted for clarity.

compound in an analytically pure form. Hence **3** was partially characterised by NMR spectroscopy and mass spectrometry.

The resonance of the amido proton was observed as an extremely broad peak centred on δ 9.0. The resonances of the protons of the other groups in the molecule were also observed to be broad at room temperature, with peak widths ($\Delta\nu_{\frac{1}{2}}$) up to 17 Hz. These peaks sharpened upon heating the sample to 80 °C. A variable temperature NMR study of **3** was performed (see below). The ^{1}H NMR spectrum is consistent with the formation of $[Nb(\eta\text{-}C_5H_5)\{N(C_6H_3Me_2\text{-}2,6)\}\{NH(C_6H_3Me_2\text{-}2,6)\}Cl]$, with two inequivalent aryl rings being observed. The ^{13}C-{^{1}H} NMR spectrum is also consistent with the proposed formulation. The assignment of the peaks between the amido and imido ligands in **3**, and both **4** and **7**, was made *via* NOE and ^{1}H–^{1}H COSY spectroscopy.

The reaction between compound **1** and a slurry of two equivalents of $LiNH(C_6H_3Me_2\text{-}2,6)$ in toluene at −78 °C, followed by slow warming to room temperature, afforded $[Nb(\eta\text{-}C_5H_5)\{N(C_6H_3Me_2\text{-}2,6)\}\{NH(C_6H_3Me_2\text{-}2,6)\}_2]$ **4** as highly air- and moisture-sensitive yellow crystals. Two formulations are possible for **4**, either the bis-amide $[Nb(\eta\text{-}C_5H_5)\{N(C_6H_3Me_2\text{-}2,6)\}\{NH(C_6H_3Me_2\text{-}2,6)\}_2]$ or the bis-imide $[Nb(\eta\text{-}C_5H_5)\{N(C_6H_3Me_2\text{-}2,6)\}_2\{NH_2(C_6H_3Me_2\text{-}2,6)\}]$. The transfer of an α-proton to form a bis-imide species has been proposed to occur in the formation of $[Nb\{N(C_6H_3{}^iPr_2\text{-}2,6)\}_2Cl(py)]$ from the reaction between $[Nb(NEt_2)_2Cl_3(OEt_2)]$ and $LiNH(C_6H_3\text{-}{}^iPr_2\text{-}2,6)$.[10] The ^{1}H NMR spectrum of **4** contains two sets of resonances assignable to the aryl groups, consistent with either of the formulations above. However NOE spectroscopy showed a correlation between the NH resonance and that of the methyl resonance integrating as 12 protons, consistent with the formulation of **4** as a bis-amido species. Also the addition of the strong σ donor trimethylphosphine did not lead to displacement of a co-ordinated amine molecule.

In order to investigate the nature of compound **4** in the solid state crystals of it suitable for a crystal structure determination were grown by layering a toluene solution of **4** with pentane. The unit cell contained four molecules, with two molecules in the asymmetric unit. There was essentially no difference in the bond lengths and angles between the two molecules, however the cyclopentadienyl ring in the molecule containing Nb(2) was found to exhibit disorder such that two ring orientations exist, each having 50% site occupation. The atom C(52) is common to both ring orientations and so has 100% site occupation.

The molecular structure of compound **4** is shown in Fig. 2 and selected interatomic distances and angles are listed in Table 3. The compound is found to exist as a bis-amide in the solid state. The imido and amido ligands have structurally distinct Nb–N–C linkages, distinguishable by differences in both the Nb–N bond lengths and the Nb–N–C bond angles. The molecules containing Nb(1) and Nb(2) crystallise as enantiomers. The two amido groups are oriented such that the aryl ring of one is directed toward the cyclopentadienyl ligand and the other is directed away, making the two groups inequivalent in the solid state.

Table 3 Selected interatomic distances (Å) and angles (°) for $[Nb(\eta\text{-}C_5H_5)\{N(C_6H_3Me_2\text{-}2,6)\}\{NH(C_6H_3Me_2\text{-}2,6)\}_2]$ **4**

Nb(1)–N(31)	1.776(5)	Nb(2)–N(81)	1.764(5)
Nb(1)–N(21)	2.016(5)	Nb(2)–N(61)	2.024(5)
Nb(1)–N(41)	2.024(5)	Nb(2)–N(71)	2.011(5)
N(31)–C(32)	1.383(7)	N(81)–C(82)	1.396(8)
N(21)–C(22)	1.398(8)	N(61)–C(62)	1.408(8)
N(41)–C(42)	1.398(8)	N(71)–C(72)	1.406(8)
Nb(1)–C(11)	2.422(7)	Nb(2)–C(51)	2.491(9)
Nb(1)–C(12)	2.462(6)	Nb(2)–C(52)	2.468(8)
Nb(1)–C(13)	2.523(6)	Nb(2)–C(53)	2.420(13)
Nb(1)–C(14)	2.462(6)	Nb(2)–C(54)	2.413(9)
Nb(1)–C(15)	2.410(7)	Nb(2)–C(55)	2.450(8)
Nb(2)–C(51′)	2.52(4)	Nb(2)–C(53′)	2.38(2)
Nb(2)–C(54′)	2.41(5)	Nb(2)–C(55′)	2.56(2)
Nb(1)–N(31)–C(32)	168.9(4)	Nb(2)–N(81)–C(82)	169.7(5)
Nb(1)–N(21)–C(22)	135.7(4)	Nb(2)–N(61)–C(62)	127.8(4)
Nb(1)–N(21)–H(2)	112.13(14)	Nb(2)–N(61)–H(6)	116.09(14)
C(22)–N(21)–H(2)	112.1(3)	C(62)–N(61)–H(7)	116.1(3)
Nb(1)–N(41)–C(42)	131.0(4)	Nb(2)–N(71)–C(72)	132.4(4)
Nb(1)–N(41)–H(4)	114.49(14)	Nb(2)–N(71)–H(7)	113.82(14)
C(42)–N(41)–H(4)	114.5(3)	C(72)–N(71)–H(7)	113.8(3)
Σ N(21)	359.93	Σ N(61)	359.99
Σ N(41)	359.99	Σ N(71)	360.02
N(31)–Nb(1)–N(21)	99.5(2)	N(81)–Nb(2)–N(61)	100.2(2)
N(31)–Nb(1)–N(41)	101.3(2)	N(81)–Nb(2)–N(71)	101.8(2)
N(21)–Nb(1)–N(41)	109.3(2)	N(61)–Nb(2)–N(71)	108.0(2)

The imido ligand is approximately linear in each of the enantiomers (Nb–N–C 168.9(4) and 169.7(5)°), and the Nb–N bond length (1.776(5) and 1.764(5) Å) is not significantly different from those in the other structurally characterised compounds in this work. This implies that the bonding of the imido ligand is not affected unduly by the presence of additional π donor ligands, and that the imido ligand is still best considered to act as a four electron donor to the metal centre.

The niobium–amido bond lengths are in the range 2.011(5)–2.024(5) Å, at the high end of the reported $Nb\text{–}N_{amido}$ bonds (1.935–2.102 Å),[11,12] significantly longer than those in the methylamido compound **7** described below, and $[Nb(\eta\text{-}C_5H_5)(N^tBu)(NH^tBu)Cl]$ (1.9674(12) and 1.9677(14) Å) and $[Nb(\eta\text{-}C_5H_5)\{N(C_6H_3{}^iPr_2\text{-}2,6)\}(NH^tBu)Cl]$ (1.958(3) Å).[3] This results from competition of the two amido ligands for the single remaining orbital with π symmetry with respect to these ligands, the others being involved in bonding to the cyclopentadienyl and imido ligands. This orbital lies in the ‘equatorial plane’ of the cyclopentadienyl and imido ligands, and leads to the amido ligands adopting an orientation such that the filled p orbital on the nitrogen can be involved in a π bonding interaction.[13] Thus the lone pairs of the amido ligands lie approximately in the plane containing the niobium atom and the two amido nitrogen atoms. Both of the amido nitrogen atoms are in a planar environment, with the sum of the angles around them being very close to 360°, indicating sp^2 hybridisation. The best description of these amido groups is to consider them to be donating a sum of four electrons to the metal centre, *i.e.* a mean donation of two electrons each. As described above, the amido ligands are arranged in opposite senses, with one of the aryl rings toward the cyclopentadienyl ring and the other toward the imido nitrogen, to minimise steric interactions. The angle that the lone pair makes to this plane is greater (15 and 17°) for the amido with its aryl ring oriented toward the cyclopentadienyl ligand, as compared to the amido with its aryl ring oriented away from the cyclopentadienyl group (2 and 7°).

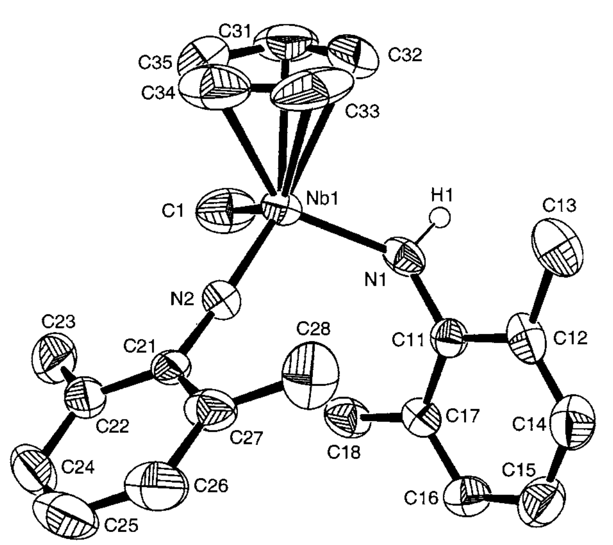

Fig. 3 The molecular structure of $[Nb(\eta\text{-}C_5H_5)\{N(C_6H_3Me_2\text{-}2,6)\}\{NH(C_6H_3Me_2\text{-}2,6)\}Me]$ **7**. Hydrogen atoms attached to carbon have been omitted for clarity.

Table 4 Selected interatomic distances (Å) and angles (°) for $[Nb(\eta\text{-}C_5H_5)\{N(C_6H_3Me_2\text{-}2,6)\}\{NH(C_6H_3Me_2\text{-}2,6)\}Me]$ **7**

Nb(1)–N(1)	1.987(6)	N(1)–C(11)	1.412(9)
Nb(1)–N(2)	1.770(6)	N(2)–C(21)	1.395(9)
Nb(1)–C(1)	2.197(8)	Nb(1)–C(33)	2.398(9)
Nb(1)–C(31)	2.500(9)	Nb(1)–C(34)	2.410(9)
Nb(1)–C(32)	2.487(9)	Nb(1)–C(35)	2.461(9)
N(2)–Nb(1)–N(2)	102.4(2)	N(2)–Nb(1)–C(1)	100.7(3)
Nb(1)–N(1)–C(11)	135.3(5)	N(1)–Nb(1)–C(1)	105.4(3)
Nb(1)–N(1)–H(1)	112.3(2)	Nb(1)–N(2)–C(21)	170.2(5)
C(11)–N(1)–H(1)	112.3(2)	Σ N(1)	359.9

As with other imido compounds the cyclopentadienyl ring in the non-disordered molecule is positioned such that one carbon nearly eclipses the niobium–imido bond. The ring is tilted toward this side, making the bonds to this carbon and one of its neighbours the shortest, and the bond to the carbon *trans* to these two the longest. The intra-ring C–C bond lengths show no significant deviation from regularity.

The reaction between $Mg(C_5H_5)_2$ and $[Nb(\eta\text{-}C_5H_5)\{N(C_6H_3Me_2\text{-}2,6)\}Cl_2]$ **1** in THF at −78 °C afforded $[Nb(\eta\text{-}C_5H_5)_2\{N(C_6H_3Me_2\text{-}2,6)\}Cl]$ **5** as red needle crystals. The reaction between **5** and LiMe afforded $[Nb(\eta\text{-}C_5H_5)_2\{N(C_6H_3Me_2\text{-}2,6)\}Me]$ **6** as orange crystals; **6** could also be obtained from the reaction between **2** and $Li(C_5H_5)$ in THF at room temperature. The addition of a solution of AgO_3SCF_3 in benzene to a solution of **5** in the same solvent yielded an intensely coloured, insoluble blue solid that proved to be intractable.

The reaction between $[Nb(\eta\text{-}C_5H_5)\{N(C_6H_3Me_2\text{-}2,6)\}MeCl]$ **2** and a slurry of one equivalent of $LiNH(C_6H_3Me_2\text{-}2,6)$ in toluene at −78 °C afforded $[Nb(\eta\text{-}C_5H_5)\{N(C_6H_3Me_2\text{-}2,6)\}\{NH(C_6H_3Me_2\text{-}2,6)\}Me]$ **7** as yellow crystals. The layering of a toluene solution of **7** with pentane afforded large yellow crystals of suitable quality for X-ray diffraction. The crystal structure of **7** has been determined. The molecular structure is shown in Fig. 3 and selected interatomic distances and angles are in Table 4.

The asymmetric unit contains only one of the enantiomers of compound **7**; the other is generated by the centre of inversion present in space group $P2_1/c$. As was the case for **4**, **7** contains structurally distinct imido and amido ligands. The imido ligand is approximately linear (Nb(1)–N(2)–C(21) 170.2(5)°), with the aryl group bent slightly toward the cyclopentadienyl ring. The Nb(1)–N(2) bond length of 1.770(6) Å is similar to that of **1**, thus the nitrogen atom of this ligand can still be considered to act as a four electron donor. The niobium–amido bond length of 1.987(6) Å is noticeably shorter than those of **4**. The sum of the angles about the amido nitrogen (359.9°) implies sp^2 hybridisation at the amido nitrogen atom, with the lone pair being involved in an interaction with the metal centre. The lone pair of the amido group is also angled slightly out of the plane of the niobium, nitrogen and methyl carbon atoms, in this instance the angle to the plane is approximately 18°.

Variable temperature NMR studies

The broad peaks observed in the room temperature ^1H NMR spectrum of $[Nb(\eta\text{-}C_5H_5)\{N(C_6H_3Me_2\text{-}2,6)\}\{NH(C_6H_3Me_2\text{-}2,6)\}Cl]$ **3** implied the presence of one or more dynamic processes in the molecule. To investigate these a variable temperature ^1H NMR study was performed, over the range +80 to −90 °C.

At 80 °C all of the peaks consisted of 3 singlets for protons of the cyclopentadienyl ring (δ 5.75), the methyl groups on the aryl rings of the amido ligand (δ 2.34) and the imido ligand (δ 2.22). The resonance due to the NH proton was observed as a slightly broadened singlet at δ 8.97. Those of the aryl protons of the amido and imido ligands were observed as a doublet and a triplet for each ring.

As the sample was cooled a number of changes were observed in the spectrum (Table 5). All of the peaks become progressively broader, and decoalesce to give two new peaks, with a ratio of approximately 0.75 : 0.25. Below this coalescence temperature the resonances of the amido proton, cyclopentadienyl group and the methyl groups of the amido ligand undergo no further changes, except to become sharper. Some temperature dependence of the position of the resonances was also observed. However, the peaks due to the protons of the methyl groups on the aryl ring of the imido ligand undergo a further broadening and decoalescence. For the major conformer decoalescence is observed at −45 °C, with two peaks of equal intensity being observed at low temperature (δ 2.57 and δ 1.76). The minor conformer has a coalescence temperature of −90 °C; the low temperature limit is not reached. Broadening and decoalescence of the aryl protons is also observed.

The crystal structures of $[Nb(\eta\text{-}C_5H_5)(N^tBu)(NH^tBu)Cl]$, the bis-amido compound **4** and the methylamido compound **7** all show that the lone pair of the amido ligand preferentially lies in the equatorial binding plane of the cyclopentadienyl and imido ligands, a conformation that arises due to the π bonding interaction of the lone pair with the niobium centre. If rotation about the $Nb\text{–}N_{amido}$ bond becomes slow on the NMR timescale then two conformers will be observed, one with the amido proton oriented toward the cyclopentadienyl ring and one with it oriented away.

The changes in the ^1H NMR spectrum can thus be explained as follows. The rotation about the $Nb\text{–}N_{amide}$ bond becomes slow on the NMR timescale, leading to the observation of two conformers. One of these has a higher energy than the other, as they have different steric requirements, leading to different concentrations of the two conformers in the sample. This explains the first decoalescence observed for each of the four singlets described above. The second decoalescence, which occurs only for the aryl rings of the imido group, results from rotation about the $N_{imido}\text{–}C_{ipso}$ bond becoming slow on the NMR timescale. The barrier to rotation about this bond in each of the conformers is different, leading to the different temperatures of coalescence.

The dynamic processes in compound **3** were modelled using the gNMR [14] package to obtain a series of rates for the different processes. From these rates the energy barrier to the rotations can be calculated from a plot of ln (k) against $1/T$. The barrier to rotation about the $Nb\text{–}N_{amido}$ bond was calculated from simulation of the cyclopentadienyl peaks, as the peaks due to

Table 5 The changes observed in the ^{1}H NMR spectrum of [Nb(η-C_5H_5){N($C_6H_3Me_2$-2,6)}{NH($C_6H_3Me_2$-2,6)}Cl] **3** as the temperature is reduced

Group	δ (High temperature)	Coalescence point/°C	δ (Major conformer)	δ (Minor conformer)
NH	8.97	25	9.23	7.92
C_5H_5	5.75	5	5.76	5.53
N{$C_6H_3(CH_3)_2$}	2.34	10	2.45	2.08
NH{$C_6H_3(CH_3)_2$}	2.22	−5	2.34	2.21

Table 6 The changes observed in the ^{1}H NMR spectrum of [Nb(η-C_5H_5){N($C_6H_3Me_2$-2,6)}{NH($C_6H_3Me_2$-2,6)}Me] **7** as the temperature is reduced

Group	δ (High temperature)	Coalescence point/°C	δ (Major conformer)	δ (Minor conformer)
NH	8.18		8.47	?[a]
C_5H_5	5.74	5	5.43	5.25
NH{$C_6H_3(CH_3)_2$}	2.35	−34	2.49	2.13
N{$C_6H_3(CH_3)_2$}	2.15	−38	2.34	2.08
$NbCH_3$	1.01	−68	1.11	1.10

[a] Obscured by the resonances of the protons of the aryl rings.

the amido proton were too broad to be simulated accurately, whilst there was considerable overlap of the peaks in the methyl region. The value obtained from this simulation was $\Delta G^\ddagger = 60.6 \pm 4$ kJ mol^{-1}. The barrier to rotation about the N_{imido}–C_{ipso} bond of the major isomer was calculated from simulation of the peaks due to this group, which fortunately was little affected by the overlaps present, giving $\Delta G^\ddagger = 45.9 \pm 3$ kJ mol^{-1}. No accurate calculation of the barrier to rotation about this bond in the minor isomer could be made as the low temperature limit was not reached. However, an approximate barrier of $\Delta G^\ddagger \approx 34$ kJ mol^{-1} can be calculated from the temperature of coalescence and estimated positions of the two resonances at the low temperature limit. The energy barriers to the rotation of these groups, and those measured for compounds **4** and **7**, are listed in Table 7 (see below).

The assignment of the major and minor conformers between that with the amido proton oriented toward the cyclopentadienyl ring and that with it oriented away could not be made with complete certainty. However, in the crystal structure of compound **7** the amido ligand has the aryl group oriented away from the cyclopentadienyl ring. An examination of this structure, in which the torsion angles about the Nb–N_{amido} and N_{amido}–C_{ipso} bonds were altered, whilst leaving the rest of the molecule unaffected showed the methyl groups of the aryl ring on the amido ligand to clash with the cyclopentadienyl ring. This interaction would lead to a compound with the aryl ring oriented toward the cyclopentadienyl ring being higher in energy than its conformer, explaining both the preferences seen in the crystal structure and the different concentrations of the two conformers observed in the spectra of **3**. Thus it is proposed that the major conformer is that with the amido proton oriented toward the cyclopentadienyl ring, which minimises the steric interactions present.

With the exception of the resonance of the amido proton, the ^{1}H NMR spectra of both compounds **4** and **7** contained sharp peaks at room temperature. However, it was believed that processes similar to those observed for **3** would also occur in these species. Accordingly low temperature NMR studies were also performed on these complexes.

On cooling a sample of compound **4** in d_8-toluene to −90 °C the resonance due to the methyl groups of the amido ligand merged into the baseline, with decoalescence occurring at −80 °C. As for **3** this broadening is likely to arise from rotation about the niobium–amido bond becoming slow on the NMR timescale. At −90 °C two broad peaks approximately centred upon δ 2.1 and 2.6 are observed. Consideration of the structure of **4** shows that three possible conformers exist. If these are labelled in terms of the orientation of the aryl ring they can be thought of as ‘up, up’, ‘up, down’ and ‘down, down’ (the conformation observed in the crystal structure is ‘up, down’). The presence of all three conformers in solution would be expected to give rise to four separate signals for the amido groups, however as the low temperature limit was not reached in this experiment only two broad peaks were observed. Two explanations for this can be envisaged. First these peaks may each consist of two overlapping signals, secondly only the ‘up, down’ conformer may be present in significant concentrations due to steric demands of placing both amido groups in the same orientation. Since the low temperature limit was not reached it is not possible to determine which of these is the case. However, a guesstimate of $\Delta G^\ddagger \approx 37$ kJ mol^{-1} for the rotation of the amido groups can be made if the second case is assumed to be true.

Table 7 Energy barriers to rotation measured for compounds **3**, **4** and **7**

Compound	$\Delta G^\ddagger$ (Nb–N_{amide})/ kJ mol^{-1}	$\Delta G^\ddagger$ (N_{imide}–C_{ipso})/kJ mol^{-1}
3	60.6 ± 4	45.9 ± 3 (major conformer) 34 (minor conformer)[a]
4	47.4 ± 2.5	
7	37[a]	

[a] Estimated value.

In a variable temperature NMR study of compound **7** all of the resonances were observed to decoalesce to give a major and a minor conformer in the approximate ratio 0.76 : 0.24, as was the case for **3**. These changes are listed in Table 6. A further decoalescence of the peak due to slowing of the rotation about the N_{imido}–C_{ipso} bond of the major isomer is observed, at a temperature of approximately −80 °C. The overlap of this peak with the peak due to residual $C_6D_5CD_2H$ means that an accurate coalescence point cannot be determined. In addition the low temperature limit is not reached.

The changes in the resonances of the protons in the cyclopentadienyl and methyl groups were simulated using the gNMR[14] package, allowing the barrier to rotation about the Nb–N_{amido} bond to be calculated as $\Delta G^\ddagger = 47.4 \pm 2.5$ and 45.6 ± 6.1 kJ mol^{-1} respectively.

The barrier to rotation about the Nb–N_{amido} bond was found to be significantly different for each of the three compounds [Nb(η-C_5H_5){N($C_6H_3Me_2$-2,6)}{NH($C_6H_3Me_2$-2,6)}X] (X = Cl **3**, NH($C_6H_3Me_2$-2,6) **4** or Me **7**). The steric bulk of the substituents X is in the order NH($C_6H_3Me_2$-2,6) > Cl > Me, thus an argument based solely on the steric requirements of the ligand X cannot explain these values and the explanation is likely to lie with electronic effects.

The crystal structures of compounds **4** and **7** show the lone pairs of the amido ligands to lie in the equatorial binding plane of the imido and cyclopentadienyl groups. This is the orientation in which π donation from the amido ligand to the niobium centre is maximised.[13] Rotation of the amido ligand away from this position will lead to a loss of the π bonding interaction, this will provide an electronic barrier to rotation of the amido ligand. This explains the low energy barrier to rotation of the amido ligands observed in **4**. The two amido ligands can only donate four electrons to the metal centre between them. If each amido ligand is considered to be donating an average of 1 π electron the loss of the π bonding interaction on rotation of an individual amido ligand will be much reduced over that in **3** and **7**. Additionally, if the rotations of the two amido groups are out of phase with one another then the loss of π interaction from one ligand can be somewhat counterbalanced by the other.

The rotation barrier in compound **3** is greater than that in **7**, despite the chloride group being a π donor whereas the methyl group is not. The amido group is clearly a far stronger π donor than the chloride, and the difference between methyl and chloro groups can be assigned to their electronegativities. This is borne out by our previous work comparing the complexes [Nb(η-C_5H_5)(N^{t}Bu)(NH^{t}Bu)Cl], [Nb(η-C_5H_5)(N^{t}Bu)(NH^{t}Bu)Me] and [Nb(η-C_5H_5)(N^{t}Bu)(NH^{t}Bu)$_2$].[3a] The difference between the chemical shifts of the α and β carbons of the *tert*-butyl groups of the amido ligands was used to infer the degree of electron donation to the niobium centre, a technique that has long been proposed for *tert*-butylimido ligands.[1] This placed the complexes in the order [Nb(η-C_5H_5)(N^{t}Bu)(NH^{t}Bu)Cl] > [Nb(η-C_5H_5)(N^{t}Bu)(NH^{t}Bu)Me] > [Nb(η-C_5H_5)(N^{t}Bu)(NH^{t}Bu)$_2$], just as has been found for the order of rotational barriers of **3**, **4**, and **7**.

The energy barriers for rotation about the Nb–N_{amido} bonds are comparable to others reported for similar Group V amido compounds. The compound [V(η-C_5H_5)(N^{t}Bu){N(SiMe$_3$)$_2$}Cl] was reported to have a barrier to rotation about the metal–amido bond of $\Delta G^‡ = 61.7$ kJ mol^{-1}.[15] The resonance of the amido methyl groups in [Nb{(η-C_5H_4)CMe$_2$(η^1-C_5H_4)}{N-(C_6H_3^{i}Pr$_2$-2,6)}(NMe$_2$)] was reported to disappear into the baseline at 20 °C and to decoalesce as two singlets at δ 2.04 and 3.58 at −80 °C (400 MHz).[12] If 20 °C is taken as the temperature of coalescence then an estimate of $\Delta G^‡ = 54.1$ kJ mol^{-1} can be made for the barrier to rotation about the metal–amido bond.

More detailed studies were made upon the systems [Ta(η-C_5Me_5){N($C_6H_3Me_2$-2,6)}(NR$_2$)X] (R = Me, X = Cl (**A**) or Me (**B**); R = ^{i}Pr, X = Me (**C**)). The variable temperature NMR spectra of these three compounds show features similar to those in the spectra of **3** and **7**. In all three cases the rotation about the Ta–N_{amido} bond became slow on the NMR timescale; lineshape analysis enabled energy barriers of $\Delta G^‡ = 50.2$, 45.1 and 58.1 kJ mol^{-1} to be calculated for **A**, **B**, and **C** respectively.[4]

The slowing of the exchange of the two methyl groups on the aryl ring of the imido ligand was also observed in these compounds, as it was for **3**, with energy barriers of $\Delta G^‡ = 44.7$ and 44.3 kJ mol^{-1} for **A** and **B** respectively. The methyl groups on the imido ligand remained inequivalent in compound **C** at all temperatures. The proposed explanation of this effect involved co-ordination of a solvent molecule (d$_2$-dichloromethane) to form a five-co-ordinate species, which then underwent a Berry pseudo-rotation to exchange the two methyl groups on the aryl ring. This had been proposed previously by the same authors to explain similar exchange processes in [Ta(η-C_5Me_5)-{N($C_6H_3Me_2$-2,6)RCl] (R = CH$_2$CMe$_2$Ph (**D**), CH$_2$CMe$_3$ (**E**) or CH$_2$C$_6$H$_5$ (**F**)) in which the energy barriers were calculated as $\Delta G^‡ = 56.4$, 53.9 and 50.2 kJ mol^{-1} respectively.[16] The differences between the energy barriers in all of these compounds were explained as being due to the different steric bulk of the substituents hampering the exchange process.

The exchange of the two methyl groups on the aryl ring of the imido ligand *via* a Berry pseudo-rotation appears unlikely to occur in compounds **3**, **4** and **7**. First these are already 18 electron compounds if the lone pair of the amido ligand is involved in the bonding to the niobium centre; **4** also has an additional lone pair present upon the amido ligands. Secondly, the solvent used in this study is d$_8$-toluene, the co-ordination of which to the niobium centre is unlikely both on electronic and steric grounds. In view of this a simple explanation involving slowing of the rotation about the N–C_{ipso} bond adequately explains the changes observed in the ^{1}H NMR spectra of **3**, **4**, and **7**.

The different energy barriers to rotation about the N_{imido}–C_{ipso} bond in each of the two conformers of compounds **3** and **7** will most likely be affected by both electronic and steric factors. The former will arise from the overlap between the π systems of the aryl ring and the Nb–N_{imido} bond. The main factor affecting the latter will be the steric bulk of the other ligands in the molecule. The observed barriers are consistent with the assignment of the major and minor isomers made previously. The major conformer has the aryl ring of the amido ligand oriented to point away from the cyclopentadienyl ring, and this hinders rotation of the aryl ring of the imido group. The minor conformer has the proton of the amido group oriented away from the cyclopentadienyl ring, and thus much less steric hindrance to rotation of the aryl ring of the imido ligand. The barriers of 45.9 ± 3 and ≈34 kJ mol^{-1} measured for **3** are lower than those measured in the d^2 molybdenum complexes [Mo{N(C_6H_2Me$_3$-2,4,6)}(CN^{t}Bu)(PMe$_3$)$_2$Cl$_2$] and [Mo{N(C_6H_2Me$_3$-2,4,6)}-(PhCCPh)(PMe$_3$)$_2$Cl$_2$] (51 and 57 kJ mol^{-1} respectively), in which the difference in energy barriers was attributed solely to steric effects.[17] It is clear the major contribution to the difference in energy barriers between the major and minor conformers of **3** can be attributed to steric interactions; an assessment of the electronic contributions to the barrier could not be made as the low temperature limit for these rotations was not reached in either **4** or **7**. An analysis of the rotation of arylimido groups in tungsten complexes using density functional theory was also recently reported.[18]

Experimental

All manipulations of air- and/or moisture-sensitive materials were performed under an inert atmosphere of dinitrogen using standard Schlenk line techniques, or in an inert atmosphere dry box containing dinitrogen. Solvents were dried over the appropriate drying agent and distilled under nitrogen. Deuteriated solvents were dried over potassium and vacuum distilled prior to use.

The compounds [Nb(η-C_5H_5)Cl$_4$][19] and [Mg(C_5H_5)$_2$][20] were prepared according to literature procedures. Lithium (2,6-dimethylphenyl)amide was prepared *via* the reaction between 2,6-dimethylaniline and *n*-butyllithium in pentane. (2,6-Dimethylphenyl)trimethylsilylamide was prepared from the reaction of trimethylsilyl chloride with a slurry of the lithium salt in pentane, and distilled before use. The compounds NbCl$_5$, 2,6-dimethylaniline, 2,6-dimethylpyridine and solutions of LiMe in diethyl ether, Li^{n}Bu in hexanes and MgMeCl in ether were purchased from the Aldrich chemical company. The amine and pyridine were dried over calcium hydride and distilled prior to use, NbCl$_5$ was purified by sublimation at 80 °C, 10^{-3} mbar. All other compounds were used as received.

NMR spectra were recorded on a Varian Unity Plus 500 spectrometer (^{1}H and ^{13}C at 499.988 and 125.718 MHz respectively) at room temperature in d$_6$-benzene unless otherwise stated, referenced internally using the residual protio solvent (^{1}H) and solvent (^{13}C) resonances and measured relative to tetramethylsilane (^{1}H and ^{13}C; $\delta = 0$). Electron impact mass spectra were recorded by the mass spectrometry service of the Dyson Perrins Laboratory in Oxford. Elemental analyses were provided by the elemental analysis department of the Inorganic Chemistry Laboratory.

Preparations

$[Nb(\eta\text{-}C_5H_5)\{N(C_6H_3Me_2\text{-}2,6)\}Cl_2]$ 1. A colourless solution of $(Me_3Si)NH(C_6H_3Me_2\text{-}2,6)$ (3.22 g, 16.67 mmol) and 2,6-dimethylpyridine (1.94 ml, 16.67 mmol) in dichloromethane (20 ml) was added dropwise to a stirred suspension of $[Nb(\eta\text{-}C_5H_5)Cl_4]$ (5 g, 16.67 mmol) in dichloromethane (50 ml). Fuming occurred during the addition, and the solution became bright red. The reaction mixture was stirred for 12 hours after which time it had darkened. The volatiles were removed under reduced pressure and the resulting red solid was extracted into toluene (3 × 30 ml) to give a dark red solution and an off-white residue. The mixture was filtered to remove $H_3N(C_6H_3Me_2\text{-}2,6)Cl$, and concentrated to 15 ml under reduced pressure. Cooling to −80 °C yielded the product as red crystals which were isolated by filtration, washed with pentane (10 ml), and dried *in vacuo*. Yield 2.7 g, 46.5% based on $[Nb(\eta\text{-}C_5H_5)Cl_4]$.

$[Nb(\eta\text{-}C_5H_5)\{N(C_6H_3Me_2\text{-}2,6)\}MeCl]$ 2. A red solution of $[Nb(\eta\text{-}C_5H_5)\{N(C_6H_3Me_2\text{-}2,6)\}Cl_2]$ (1.00 g, 2.87 mmol) in diethyl ether (20 ml) was cooled to −78 °C. To this was added a solution of MgMeCl in diethyl ether (0.95 ml of a 3 M solution, 2.85 mmol). The reaction was stirred at −78 °C for 30 minutes, allowed to warm slowly to room temperature and stirred for 3 hours. The volatiles were removed under reduced pressure and the resulting red solid was extracted with pentane (3 × 10 ml) to give a red solution and a white residue. The combined extracts were then concentrated to 10 ml under reduced pressure and cooled to −80 °C to afford the product as red crystals which were isolated by filtration, washed with cold pentane (10 ml) and dried *in vacuo*. Yield 0.89 g, 94.5% based on $[Nb(\eta\text{-}C_5H_5)\{N(C_6H_3Me_2\text{-}2,6)\}Cl_2]$.

$[Nb(\eta\text{-}C_5H_5)\{N(C_6H_3Me_2\text{-}2,6)\}\{NH(C_6H_3Me_2\text{-}2,6)\}Cl]$ 3. A red solution of $[Nb(\eta\text{-}C_5H_5)\{N(C_6H_3Me_2\text{-}2,6)\}Cl_2]$ (0.500 g, 1.44 mmol) in toluene (80 ml) was cooled to −78 °C and added dropwise to a pre-cooled slurry of $LiNH(C_6H_3Me_2\text{-}2,6)$ (0.183 g, 1.44 mmol) in toluene (20 ml). The mixture was stirred at low temperature for 1 hour, allowed to warm up slowly over 3 hours, and then stirred for 3 hours. Over this time the reaction mixture became a paler red, and a white precipitate formed. The volatiles were then removed under reduced pressure and the resulting orange solid was extracted into toluene (3 × 10 ml). The combined extracts were concentrated to 15 ml under reduced pressure and cooled slowly to −20 °C to give the product as a yellow solid, which was isolated by filtration, washed with cold pentane (2 × 10 ml) and dried *in vacuo*. Yield 0.53 g, 85.0% based on $[Nb(\eta\text{-}C_5H_5)\{N(C_6H_3Me_2\text{-}2,6)\}Cl_2]$.

$[Nb(\eta\text{-}C_5H_5)\{N(C_6H_3Me_2\text{-}2,6)\}\{NH(C_6H_3Me_2\text{-}2,6)\}_2]$ 4. A red solution of $[Nb(\eta\text{-}C_5H_5)\{N(C_6H_3Me_2\text{-}2,6)\}Cl_2]$ (1.00 g, 2.87 mmol) in toluene (30 ml) was cooled to −78 °C and added dropwise to a pre-cooled slurry of $LiNH(C_6H_3Me_2\text{-}2,6)$ (0.73 g, 5.74 mmol) in toluene (120 ml). The mixture was stirred at low temperature for 1 hour, allowed to warm slowly to room temperature over 3 hours, and then stirred for 3 hours. Over this time it became orange and a white precipitate was formed. The volatiles were then removed under reduced pressure and the resulting orange solid was extracted into toluene (3 × 20 ml) to give an orange solution. The combined extracts were concentrated to 20 ml under reduced pressure and cooled slowly to −80 °C to give the product as yellow crystals which were isolated by filtration, washed with pentane (2 × 10 ml) and dried *in vacuo*. Yield 0.71g, 47.7% based on $[Nb(\eta\text{-}C_5H_5)\{N(C_6H_3Me_2\text{-}2,6)\}Cl_2]$.

$[Nb(\eta\text{-}C_5H_5)_2\{N(C_6H_3Me_2\text{-}2,6)\}Cl]$ 5. A solution of $Mg(C_5H_5)_2$ (0.177 g, 2.30 mmol) in benzene (30 ml) was added dropwise to a stirred red solution of $[Nb(\eta\text{-}C_5H_5)\{N(C_6H_3Me_2\text{-}2,6)\}Cl_2]$ (0.8 g, 2.30 mmol) in benzene (30 ml). Over the course of the addition a white precipitate occurred. The reaction mixture was stirred for 30 minutes, after which time the volatiles were removed under reduced pressure and the resulting red solid extracted with pentane (2 × 30 ml). The combined extracts were concentrated to 15 ml under reduced pressure and cooled to −80 °C to afford the product as red crystals, which were isolated by filtration and dried *in vacuo*. The filtrate was reduced in volume to 7 ml under reduced pressure and cooled to −80 °C to yield a second crop of crystals. Yield 0.69 g, 79.7% based on $[Nb(\eta\text{-}C_5H_5)\{N(C_6H_3Me_2\text{-}2,6)\}Cl_2]$.

$[Nb(\eta\text{-}C_5H_5)_2\{N(C_6H_3Me_2\text{-}2,6)\}Me]$ 6. *Method A.* A red solution of $[Nb(\eta\text{-}C_5H_5)_2\{N(C_6H_3Me_2\text{-}2,6)\}Cl]$ (0.500 g, 1.3 mmol) was cooled to −78 °C. To this was added dropwise a solution of LiMe in Et_2O (0.9 ml of a 1.5 M solution, 1.35 mmol). The reaction mixture was stirred at low temperature for one hour and then allowed to warm slowly to room temperature. Over this time it became orange and a white precipitate was formed. The volatiles were removed under reduced pressure and the resulting orange solid was extracted with pentane (2 × 20 ml). The combined extracts were concentrated to 10 ml under reduced pressure and cooled to − 80 °C to afford the product as orange crystals, which were isolated by filtration and dried *in vacuo*. Yield 0.38 g, 81.0% based on $[Nb(\eta\text{-}C_5H_5)_2\{N(C_6H_3Me_2\text{-}2,6)\}Cl]$.

Method B. A colourless solution of $Li(C_5H_5)$ (0.110 g, 1.53 mmol) in THF (15 ml) was added dropwise to a stirred red solution of $[Nb(\eta\text{-}C_5H_5)\{N(C_6H_3Me_2\text{-}2,6)\}MeCl]$ (0.500 g, 1.53 mmol) in THF (20 ml) at room temperature. During the addition the mixture changed to orange and a white precipitate was formed. The reaction mixture was stirred for one hour, after which it was worked up as in method A. Yield 0.38 g, 69.7% based on $[Nb(\eta\text{-}C_5H_5)\{N(C_6H_3Me_2\text{-}2,6)\}MeCl]$.

$[Nb(\eta\text{-}C_5H_5)\{N(C_6H_3Me_2\text{-}2,6)\}\{NH(C_6H_3Me_2\text{-}2,6)\}Me]$ 7. A red solution of $[Nb(\eta\text{-}C_5H_5)\{N(C_6H_3Me_2\text{-}2,6)\}MeCl]$ (0.500 g, 1.53 mmol) in toluene (20 ml) was cooled to −78 °C and added dropwise to a slurry of $LiNH(C_6H_3Me_2\text{-}2,6)$ (0.194 g, 1.53 mmol) in toluene (80 ml) at −78 °C. The mixture was stirred at −78 °C for 1 hour, and then allowed to warm slowly to room temperature over four hours. During this time it changed to orange, and a white precipitate was formed. The reaction mixture was stirred for 2 hours, after which time the volatiles were removed under reduced pressure and the resulting orange solid was extracted into toluene (3 × 20 ml). The combined extracts were concentrated to 20 ml under reduced pressure and slowly cooled to −80 °C to afford the product as yellow crystals which were isolated by filtration, washed with cold pentane (2 × 5 ml) and dried *in vacuo*. Concentration of the filtrate to 7 ml and subsequent cooling to −80 °C yielded a second crop of crystals. Yield 0.39 g, 61.8% based on $[Nb(\eta\text{-}C_5H_5)\{N(C_6H_3Me_2\text{-}2,6)\}MeCl]$.

Crystallography

Data were collected for compounds **3**, **4** and **7** as previously described,[21] the images being processed with the DENZO and SCALEPACK programs.[22] All solution, refinement and graphical calculations were performed using the CRYSTALS[23] and CAMERON[24] software packages. The asymmetric unit of **4** contains two molecules in general positions and that molecule containing atom Nb(2) was found to exhibit disorder of the cyclopentadienyl ring, such that two eclipsed ring orientations exist, having 50% site occupation each. Atom C(52) is common to both ring orientations and hence has 100% site occupation. The NH amide hydrogen atoms in compounds **3** and **4** were located from the Fourier difference maps. Their positions were subsequently refined with their isotropic thermal parameters fixed at *ca.* 1.2 times the equivalent isotropic thermal parameters of the parent nitrogen atom. Crystallographic data are summarised in Table 8.

Table 8 Crystal data and structure refinement for compounds **1**, **4** and **7**

	1	**4**	**7**
Molecular formula	$C_{13}H_{14}Cl_2NNb$	$C_{29}H_{34}N_3Nb$	$C_{22}H_{27}N_2Nb$
Formula weight	348.07	517.50	412.37
Crystal system	Monoclinic	Triclinic	Monoclinic
Space group	$P2_1/n$	$P\bar{1}$	$P2_1/c$
a/Å	8.775(2)	7.969(10)	8.490(2)
b/Å	12.804(2)	17.246(20)	24.276(5)
c/Å	12.648(2)	18.845(10)	10.274(2)
α/°		76.26(6)	
β/°	103.61(2)	89.60(3)	108.29(3)
γ/°		89.97(5)	
V/Å^3	1381.1	2515.7(45)	2010.6(7)
Z	4	2	4
T/K	180	150	150
μ/mm^{-1}	1.20	0.50	0.605
Total data collected	7157	7909	2444
Unique data	2682	7866	2444
R	0.0508	0.0667	0.0553
R_w	0.0533	0.1319	0.1178

CCDC reference number 186/2247.

See http://www.rsc.org/suppdata/dt/b0/b007178l/ for crystallographic files in .cif format.

Acknowledgements

We thank the EPSRC for a studentship (M. J. H.) and St Johns College, Oxford for partial support.

References

1 W. A. Nugent, *Inorg. Chem.*, 1983, **22**, 965; W. A. Nugent and J. M. Mayer, Metal–Ligand Multiple Bonds, John Wiley & Sons, New York, 1988; D. E. Wigley, *Prog. Inorg. Chem.*, 1994, **42**, 239.

2 P. J. Walsh, F. J. Hollander and R. G. Bergman, *J. Am. Chem. Soc.*, 1988, **110**, 8729; D. S. Glueck, F. J. Hollander and R. G. Bergman, *J. Am. Chem. Soc.*, 1989, **111**, 2719; P. J. Walsh, F. J. Hollander and R. G. Bergman, *Organometallics*, 1993, **12**, 3705; K. E. Meyer, P. J. Walsh and R. G. Bergman, *J. Am. Chem. Soc.*, 1994, **116**, 2669; K. E. Meyer, P. J. Walsh and R. G. Bergman, *J. Am. Chem. Soc.*, 1995, **117**, 974; S. Y. Lee and R. G. Bergman, *J. Am. Chem. Soc.*, 1996, **118**, 6396; C. C. Cummins, C. P. Schaller, G. D. van Duyne, P. T. Wolczanski, A. W. E. Chan and R. Hoffmann, *J. Am. Chem. Soc.*, 1991, **113**, 2985; J. L. Bennett and P. T. Wolczanski, *J. Am. Chem. Soc.*, 1994, **116**, 2179; C. C. Cummins, S. M. Baxter and P. T. Wolczanski, *J. Am. Chem. Soc.*, 1988, **110**, 8731; J. de With and A. D. Horton, *Angew. Chem., Int. Ed. Engl.*, 1993, **32**, 903; J. de With and A. D. Horton, *Organometallics*, 1993, **12**, 1493; C. P. Schaller and P. T. Wolczanski, *Inorg. Chem.*, 1993, **32**, 131; P. Royo and J. Sánchez-Nieves, *J. Organomet. Chem.*, 2000, **597**, 61.

3 (*a*) M. J. Humphries, M. L. H. Green, M. A. Leech, V. C. Gibson, M. Jolly, D. N. Williams, M. R. J. Elsegood and W. Clegg, *J. Chem. Soc., Dalton Trans.*, 2000, 4044; (*b*) M. I. Alcalde, M. P. Gómez-Sal and P. Royo, *Organometallics*, 1999, **18**, 546.

4 A. Castro, M. V. Galakhov, M. Gómez and F. Sánchez, *J. Organomet. Chem.*, 1999, **580**, 161.

5 A. Antiñolo, M. Fajardo, C. Huertas, A. Otero, S. Prashar and A. M. Rodriguez, *J. Organomet. Chem.*, 1999, **585**, 154.

6 H. Yasuda, T. Okamoto and A. Nakamura, *Organomet. Synth.*, 1988, **4**, 20.

7 D. N. Williams, J. P. Mitchell, A. D. Poole, U. Siemeling, W. Clegg, D. C. R. Hockless, P. A. O'Neill and V. C. Gibson, *J. Chem. Soc., Dalton Trans.*, 1992, 739.

8 S. Schmidt and J. Sundermeyer, *J. Organomet. Chem.*, 1994, **472**, 127; V. C. Gibson, A. D. Poole, U. Siemeling and D. N. Williams, *J. Organomet. Chem.*, 1993, **462**, C12; M. C. W. Chan, J. M. Cole, V. C. Gibson, J. A. K. Howard, C. Lehmann, A. D. Poole and U. Siemeling, *J. Chem. Soc., Dalton Trans.*, 1998, 103.

9 W. A. Herrmann, G. Weichselbaumer, R. A. Paciello, R. A. Fischer, E. Herdtweck, J. Okuda and D. W. Marz, *Organometallics*, 1990, **9**, 489.

10 Y.-W. Chao, P. A. Wexler and D. E. Wigley, *Inorg. Chem.*, 1990, **29**, 4592.

11 D. J. Brauer, H. Burger, G. R. Liewald and J. Wilke, *J. Organomet. Chem.*, 1986, **310**, 317; L. G. Hubert-Pfalzgraf, M. Tsunoda and G. L. Borgne, *J. Chem. Soc., Dalton Trans.*, 1988, 533; A. Antinolo, A. Otero, F. Urbanos, S. Garcia-Blanco, S. Martinez-Carrera and J. Sanz-Aparicio, *J. Organomet. Chem.*, 1988, **350**, 25; A. A. Danopoulos, R. S. Hay-Motherwell, G. Wilkinson, T. K. N. Sweet and M. B. Hursthouse, *Polyhedron*, 1997, **16**, 1081; W. A. Herrmann, W. Baratta and W. Herdtweck, *Angew. Chem., Int. Ed. Engl.*, 1996, **35**, 1951; V. M. Visciglio, P. E. Fanwick and I. P. Rothwell, *Inorg. Chim. Acta*, 1993, **211**, 203; C. Heath and M. B. Hursthouse, *J. Chem. Soc. A*, 1971, 143; M. Polamo and M. Leskela, *J. Chem. Soc., Dalton Trans.*, 1996, 4345; M. G. Fickes, A. L. Odom and C. C. Cummins, *Chem. Commun.*, 1997, 1993; D. M. Hoffman and S. P. Rangarajan, *Acta Crystallogr., Sect. C*, 1996, **52**, 1616.

12 W. A. Herrmann, W. Baratto and E. Herdtweck, *J. Organomet. Chem.*, 1997, **541**, 445.

13 V. C. Gibson, *Angew. Chem., Int. Ed. Engl.*, 1994, **33**, 1565; J. W. Lauher and R. Hoffmann, *J. Am. Chem. Soc.*, 1976, **98**, 1729.

14 P. H. M. Budzelaar, in gNMR, Cherwell Scientific Ltd., The Magdalen Centre, Oxford Science Park, Oxford, 1995.

15 F. Preuss, H. Becker and T. Wieland, *Z. Naturforsch., Teil B*, 1990, **45**, 191.

16 A. Castro, M. V. Galakhov, M. Gómez, P. Gómez-Sal, A. Martin and P. Royo, *J. Organomet. Chem.*, 1998, **554**, 185.

17 F. Montilla, A. Galindo, E. Carmona, E. Gutiérrez-Puebla and A. Monge, *J. Chem. Soc., Dalton Trans.*, 1998, 1299.

18 G. Hogarth, D. G. Humphrey, N. Kaltsoyannis, W.-S. Kim, M.-Y. Lee, T. Norman and S. P. Redmond, *J. Chem. Soc., Dalton Trans.*, 1999, 2705.

19 H. Yasuda, T. Okamoto and A. Nakamura, *Organomet. Synth.*, 1988, **4**, 18.

20 A. W. Duff, P. B. Hitchcock, M. F. Lappert, R. G. Taylor and J. A. Segal, *J. Organomet. Chem.*, 1985, **293**, 271.

21 L. H. Doerrer, M. L. H. Green, D. Häußinger and J. Saßmannhausen, *J. Chem. Soc., Dalton Trans.*, 1999, 2111.

22 Z. Otwinowski and W. Minor, *Methods Enzymol.*, 1996, **276**, 307.

23 D. J. Watkin, C. K. Prout, J. R. Carruthers and P. W. Betteridge, *CRYSTALS User Guide, Issue 10*, Chemical Crystallography Laboratory, University of Oxford, 1996.

24 D. J. Watkin, C. K. Prout and L. J. Pearce, CAMERON, Chemical Crystallography Laboratory, University of Oxford, 1996.